

https://dspace.org/

Optimizing aboveground carbon mapping in Afrotemperate forests to fulfil IPCC carbon reporting standards

Jolene Fisher

ELSEVIER SCIENCE BV
https://hdl.handle.net/10539/42974
WOS

Downloaded from a DSpace repository. https://dspace.org/

JOURNAL ARTICLE

WITS-2024-0004659

General Information

Report Year:	2024	**Publication Year:**	2023
Title of Article:	Optimizing aboveground carbon mapping in Afrotemperate forests to fulfil IPCC carbon reporting standards		

AccreditedOrNot

Journal Title:	FOREST ECOLOGY AND MANAGEMENT
Citation Index:	WOS
ISSN Number:	0378-1127
Publisher:	ELSEVIER SCIENCE BV
Publisher Location:	NETHERLANDS

Journal/Page Details

Volume:	552	**Number:**	N/A		
Page From:	1	**Page To:**	10	**DOI**	10.1016/j.foreco.2023.121583

Contributor Details:

Internal Authors:

Sequence	Name	Surname	Staff No	Department
1	Jolene	Fisher	A0021726	School of Animal, Plant and Environmental Sciences

External Authors:

Total external authors: 0

Other Details:

Open Access Journal: YES

Funders:

BoardFieldName	ResearchFieldName
Natural sciences	Earth and related environmental sciences

Field Of Research:

FunderName	GrantNumber
National Research Foundation	117983

External Links:

Supporting Documents:

Document Type	DocumentURL
ELECTRONIC JOURNAL	http://acidalia.ds.wits.ac.za/AppNet/docpop/docpop.aspx?clienttype=html&docid=4773332

Submission:

NB! Only full length, peer reviewed articles in journals qualify for subsidy. This excludes editorials, book reviews, comments, abstracts for conferences and all short updates or opinion pieces.

Faculty

Faculty of Science

School

School of Animal, Plant and Environmental Sciences

Department
Complies with 75% Rule?
NO

Forest Ecology and Management 552 (2024) 121583



Contents lists available at ScienceDirect

Forest Ecology and Management

journal homepage: www.elsevier.com/locate/foreco

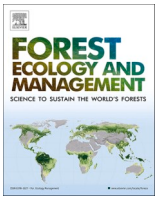



Optimizing aboveground carbon mapping in Afrotemperate forests to fulfil IPCC carbon reporting standards

Jolene T. Fisher

School of Animal, Plant and Environmental Sciences, University of the Witwatersrand, Johannesburg, South Africa

ARTICLE INFO

Keywords:
Afrotemperate forest
LiDAR
Allometry
Global biomass
Calibration and validation

ABSTRACT

Under the Paris Agreement, signatories are obliged to reduce carbon emissions and enhance carbon sinks. Multiple global aboveground biomass products are now available; however, they still require additional calibration and validation datasets at the local scale. I use South Africa's Afrotemperate forests as a case study to investigate best practice for remote sensing aboveground carbon for improving the accuracy of reporting under the Paris Agreement. I collected both field and LiDAR data for three forests in KwaZulu-Natal, South Africa, and tested three different allometric equations for calculating AGC. I used linear models to predict AGC from LiDAR data for both local and multi-site models and then compared the results with two global biomass products. The locally derived allometric produced intermediate AGC values to the temperate and pan-tropical equations and is recommended for use in South African forests. Local LiDAR models for each forest varied in performance with R^2 values ranging from 0.16 to 0.75, and RMSE% of 7.3–50%. Overall, the multi-site LiDAR model performed better than two of the three local models with a conditional pseudo-R^2 of 0.82 and RMSE on 24% (30 MgC.ha^{-1}) and is recommended in the absence of field data. However, since the forest physiognomy is diverse, it is important to take local context into account when interpreting AGC results. Although global biomass products tend to overestimate the carbon in these forests, they can still be used for the UNFCCC's 2023 global carbon stocktake until further calibration and validation data have been included. While generalized mapping techniques may produce some errors in AGC estimates, it's important to use the data that's currently available and report the uncertainty in the estimates as part of mitigating anthropogenic changes.

1. Introduction

Anthropogenic change has degraded the ability of the environment to provide critical ecosystem services including carbon sequestration (Parmesan et al., 2022). Strong evidence is available linking climate change to shifts in vegetation and biomes, affecting habitat quality, and carbon removal, emissions, and stocks (Parmesan et al., 2022). Under the Paris Agreement (2015) of the UNFCCC (United Nations Framework Convention on Climate Change), the 196 signatories are obliged to reduce carbon emissions and enhance carbon sinks. Targets to reduce the net carbon emissions include those related to greenhouse gas (GHG) emissions, indirect targets that impact on GHG emissions (increase contribution of renewable energy; reduce deforestation), and actions (change legal policies) (Fransen, 2021). Annex I countries contribute the most towards global emissions, and all but Russia have committed to significant reductions in emissions by 2030. Although their emissions are substantially lower, Non-Annex I countries including Argentina, Brazil, South Africa and South Korea have submitted revised Nationally Determined Contributions (NDC) pledging reduced emissions (Fransen, 2021).

South Africa's (SA) updated first Nationally Determined Contribution (NDC) goal for emissions is to be in a range of 398–510 $MgCO_2$ by 2025, and 350–420 by 2030 $MgCO_2$. National carbon sinks are often included in a country's GHG emissions inventory; however, measuring, mapping and monitoring carbon stocks is a subject of much debate and research globally (Duncanson et al., 2022; Kim et al., 2021). In the National Terrestrial Carbon Sinks Assessment (2020) for SA, the Total Ecosystem Organic Carbon (TEOC) is calculated by adding together the various carbon pools (soil organic carbon + above and below ground biomass for woody and herbaceous plants + biomass of above ground litter) multiplied by a carbon fraction. All carbon pools are based on the area of land covered by each biome and calculated using published carbon values for each biome, which were either estimated using fieldwork or remote sensing, and mapped at a 1 km resolution. These values therefore do not account for spatial-temporal heterogeneity in carbon storage within each biome and, at best, estimates intact,

E-mail address: Jolene.Fisher@wits.ac.za.

https://doi.org/10.1016/j.foreco.2023.121583
Received 26 September 2023; Received in revised form 8 November 2023; Accepted 9 November 2023
Available online 23 November 2023
0378-1127/© 2023 The Author(s). Published by Elsevier B.V. This is an open access article under the CC BY-NC license (http://creativecommons.org/licenses/by-nc/4.0/).

non-degraded landscapes (DEFF, 2020a).

The forest biome in South African covers 0.56% of the country (Mucina and Rutherford, 2006); however, the TEOC for forests is reported as zero (DEFF, 2020a). This is due to the fact that the models used for estimating above ground carbon do not perform well over steep terrain (Spracklen and Righelato, 2014) (many forests are on the escarpment), the models tend to saturate at 120 MgC.ha^{-1}, and due to the coarse resolution (1 km), the smaller and often non-contiguous forests are poorly mapped (DEFF, 2020a). However, Reducing Emissions from Deforestation and forest Degradation (REDD+) has been identified as a climate change mitigation strategy in the NDC (DEFF, 2020a, 2020b) and in order to participate in strategies such as REDD+ , baseline measurements, and further monitoring, of carbon are necessary (Araza et al., 2023).

Fine-scale field measurements of aboveground carbon (as estimated from aboveground biomass by a conversion factor) have only been collected for a handful of forests in South Africa (Afrotemperate forests; mistbelt forests (Mensah et al., 2017, 2016); dune forests (Mangwale et al., 2017; Rolo et al., 2018; Smithwick, 2019); and mangroves (Banda et al., 2021; Johnson et al., 2020; Steinke et al., 1995). Forests in South Africa are relatively understudied due to their inaccessibility from steep terrain or land ownership rights, and their discontinuous distribution. In addition, because these forests cover such a small area of land surface, research into the biomass of South African forests is often neglected in favour of researching the biomass of woodlands (which fall under the savanna biome) in South Africa (Bouvet et al., 2018; Colgan et al., 2013, 2012; Mograbi et al., 2015; Naidoo et al., 2015; Odipo et al., 2016), which cover a much larger (46%) extent of the country (Mucina and Rutherford, 2006) and therefore account for a larger proportion of carbon storage at a national scale. Similarly across the continent, aboveground biomass (AGB) in Afromontane and Afrotemperate forests is poorly studied and show little agreement between global AGB maps (Araza et al., 2023); however, tropical montane forests are estimated to contain a median of 254 MgC.ha^{-1} (Spracklen and Righelato, 2014) and therefore these forests should not be ignored.

Aboveground biomass is most commonly calculated using allometric equations; however, the choice of allometric equation can influence results (Ahmed et al., 2013). It is often not feasible to create specific allometric equations for each location of interest by destructively sampling a minimum of 50 trees depending on the population's size class distribution (Roxburgh et al., 2015). Therefore, one needs to choose the most appropriate allometric, or even a suite of parsimonious equations and evaluate the range of biomass that could occur in the region. Allometric equations for AGB are based on the relationship between tree stem diameter at breast height (dbh), crown height, wood density, and can also include crown dimensions (Dimobe et al., 2018; Loubota Panzou et al., 2021; Ploton et al., 2016); however, this relationship is heteroscedastic, and the error produced by the equation needs to be accounted for (Nickless et al., 2011). Additional uncertainty in biomass estimates arise when calculated from remotely sensed imagery as biomass is predicted from an aspect of the vegetation's structure, such as tree height derived from active remote sensing, which is related to forest biomass as calculated using allometric equations (Ahmed et al., 2013). The exclusion of crown dimensions in field and remotely sensed estimates can introduce bias towards large trees introducing further uncertainty in biomass estimates (Ploton et al., 2016).

Airborne Light Detection and Ranging (LiDAR) is an active remote sensing method that is used to map vegetation structure and estimate aboveground carbon (AGC) in forests globally (Lefsky et al., 2002b). To date LiDAR has been used successfully in tropical forests (Asner et al., 2012; Coomes et al., 2017; Xu et al., 2017); boreal forests (Lefsky et al., 1999a; Maltamo et al., 2005; Morsdorf et al., 2004; Vepakomma et al., 2008; Zhao et al., 2018) and deciduous forests (Lefsky et al., 2002a, 1999b). Although airborne LiDAR is frequently used for commercial purposes, the cost of commissioning data capture can be prohibitive for research and government agencies especially in the Global South. The launch of the Global Ecosystem Dynamics Investigation (GEDI) in 2018 (Dubayah et al., 2022) has resulted in a new generation of global biomass maps (Dubayah et al., 2022; Duncanson et al., 2022) as it was the first spaceborne LiDAR sensor which was specifically launched to measure ecosystem structure (Dubayah et al., 2022). Several space agencies, including NASA (National Aeronautics and Space Administration), ESA (European Space Agency) and JAXA (Japanese Aerospace Exploration Agency), have prioritized the mapping of aboveground carbon, and have produced five "global" biomass products with varying accuracies due to different spatial resolutions and sensor types (https://www.earthdata.nasa.gov/maap-biomass/). To improve accuracy, global biomass projects also use locally collected field and airborne LiDAR data to calibrate and validate their models (Duncanson et al., 2022)(https://ceos.org/gst/jpl--biomass.html; https://ceos.org/gst/africa-biomass.html; https://climate.esa.int/en/projects/biomass/about/), resulting in better accuracy for regions and biomes with more local data. In 2023, the UNFCCC will perform its first "Global Stocktake" of aboveground carbon, further highlighting the importance of global biomass mapping. Even though the scientific community is mapping AGB globally, many products do not show agreements with country's National Forest Inventory (NFI) data or with the United Nation's Forest Resource Assessment (FRA) (Araza et al., 2023).

I use South Africa's Afrotemperate forests as a case study to investigate best practice for remote sensing aboveground carbon for improving the accuracy of global biomass datasets. I address the following questions: 1. Which allometric equations should be used for South Africa's temperate forests? 2. Can models relating field measured AGC to LiDAR estimated canopy height be generalised across forest patches? Finally, I compare the results with those of two global biomass products and discuss the way forward for quantifying AGC of these forests in sub-Saharan Africa for national inventories and reporting.

2. Methods

2.1. Study sites

Afrotemperate forests occur non-randomly in the landscape. They are found on steep south facing slopes within a grassland matrix, where they are protected from fires. Afrotemperate forests occur as an archipelago over extent range of 400 km and are typically small in size (mean size = 16.0 ha, median size = 2.6 ha; (Adie et al., 2013). The study region (Fig. 1) experiences seasonal rainfall with mean annual precipitation increasing from west (Umgano – 1100 mm) to east (Karkloof – 1600 mm) (Mucina and Rutherford, 2006). Average temperatures for these forests range from 10 °C in July to 19 °C in the hottest months (January) (Mucina and Rutherford, 2006). Dargle and Karkloof forests are both secondary forests while Umgano is considered a primary forest patch. Widespread logging was practiced during the mid-1800 s to early 1900′s as evidenced by sawpits and sliptrails (H.G. FOURCADE, 1889; Lawes et al., 2007; Lawes and Eeley, 2000; McCracken, 1986) and as a result, very few primary forests remain. Secondary forest is defined here as vegetation that shows the structural or compositional legacy of a prior disturbance event (Corlett, 1994) whereas the species found in primary forest are those indicative of a late successional stage where climax vegetation is self-perpetuating. Secondary forests are dominated by long-lived angiosperms which were the colonising cohort of trees post-logging and show little regeneration under the canopy as they are light-demanding; whereas primary Afrotemperate forests are dominated by shade tolerant Podocarps (Podocarpaceae) which are often more than 100 years old and can store up to double the amount of carbon of a secondary forest (Adie et al., 2013).

2.2. Ground truthing of above ground carbon (AGC)

We collected field inventory data in the three sites from 2016 to 2019 (Dargle: November 2016, 15 plots; Karkloof: September 2017, March 2018, June 2019, 16 plots; Umgano: July 2019, 13 plots). In each

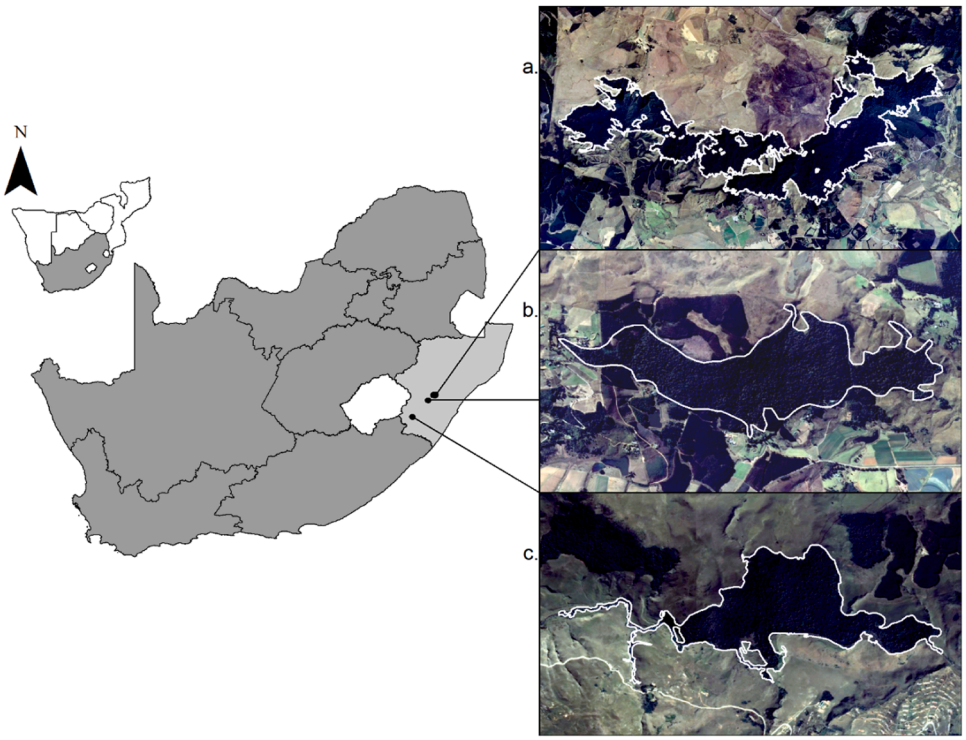

Fig. 1. Study sites in KwaZulu-Natal, South Africa. a. Karkloof Forest, b. Dargle Forest and c. Umgano forest.

circular plot (30 m radius, 0.28 ha) we measured stem diameter (at breast height, 1.3 m, dbh), stem number, tree height and species identity of all living trees with a dbh > 20 cm within the entire plot, and trees with a dbh 2.5 – 20 cm within a 0.071 ha centrally located sub-plot (15 m radius), except in Dargle forest where we only measured trees > 20 cm. From preliminary fieldwork in the Dargle forest, where we enumerated all stems ≥ 10 cm dbh in five 0.28 ha plots, we established that trees < 20 cm dbh contributed < 3% of stand biomass. Consequently, we only measured stems > 20 cm dbh and increased plot size because precision in AGC estimation increases with plot size (Zolkos et al., 2013). (Mascaro et al., 2011) investigated the error in AGC for different plot sizes and when crown placement (if the crown occurred within or outside the plot) was taken into account to relate field measured AGC and LiDAR estimated AGC, error for a plot of 0.25 ha was found to be 16.2 MgC.ha^{-1} (15%); when crown placement was not taken into account, as in this study, RMSE was 20.6 MgC.ha^{-1}(19%). Each tree > 20 cm DBH was uniquely tagged for future reference. Tree height for each individual was measured using a laser distance meter (Leica DISTO™ D510) or laser rangefinder (TruPulse™ 360° B). A Trimble (Trimble® Recon® Handheld with ProXRS antenna) differential GPS was used to collect the coordinates of the plot centre; points were then differentially corrected to sub-meter accuracy using the Pietermaritzburg trigonometric base station one second data (http://www.trignet.co.za/). The relationship between stem dbh and height was established using power law (Chave et al., 2014; Mensah et al., 2018).

Above ground biomass was calculated for each tree (each stem of multi-stemmed trees were treated as a single tree) using three different allometric equations (see below) for comparison with published data on AGB in Afrotemperate forests. Eq. 1 was derived from a set of 50 trees destructively sampled by (Beets, 1980) in a temperate rain forest in New Zealand and included species of Podocarpaceae (Coomes et al., 2002). Chave et al. (2014) developed Eq. 2 from a dataset of 4004 trees from lowland and montane tropical forests in the Americas, Africa, Asia, and Australia and is the most extensive pantropical allometric to date. In 2016 Mensah et al. (2016) developed an allometric equation (Eq. 3) specifically for mistbelt forests in South Africa. The authors collected data non-destructively from 59 individuals of four species, with *Combretum kraussii* being common between the sampled mistbelt forests, and the Afrotemperate forests considered in this study (Mensah et al., 2016). All three allometric equations contain a height parameter which improves the precision of biomass estimates (Chave et al., 2005).

$$AGB = 0{\cdot}0000598\rho(d^2H)^{0{\cdot}946}(1–0{\cdot}0019d) + 0{\cdot}03d^{2{\cdot}33} + 0{\cdot}0406d^{1{\cdot}53} \quad (1)$$

(Coomes et al., 2002).

$$AGB = 0{\cdot}0673 \text{ x } (\rho d^2H)^{0{\cdot}976} \quad (2)$$

(Chave et al., 2014).

$$\ln AGB = -2{\cdot}69 + 0{\cdot}69\ln\rho + 0{\cdot}95\ln(d^{\,2} x\, H\,) \quad (3)$$

(Mensah et al., 2016).

Where H is tree height (m), d is dbh (cm), and ρ is species-specific wood density (measured in kg m^{-3} for Eq. 1, and g cm^{-3} in Eqs. 2 and 3). It was important to use allometric equations which include height, as height is the metric that correlates to the LiDAR data. Wood density values were taken from a global database (Chave et al., 2009; Zanne et al., 2009); mean genus values were used if the species value was not available (Marshall et al., 2012). If no value was available, a generic value of 580 kg.m^{-3} was used (Chave et al., 2005). Biomass was then converted to AGC by multiplying by 0.47 (Martin and Thomas, 2011).

2.3. Light detection and ranging (LiDAR)

Small footprint, discrete return LiDAR data were collected over the Dargle forest in June 2016 and over Karkloof and Umgano forests in June 2018 (Table 1). Since the forests are predominantly evergreen, the time gap between LiDAR data collection and field data collection did not affect phenology, quality of ground truthing data, or quality of the LiDAR data. The first LiDAR return typically indicates the top of canopy vegetation (or ground if it is the sole return), and the last return indicates ground, unless dense vegetation is present. The point cloud was processed using LASTools to create a Digital Elevation Model (DEM - ground) and a Digital Surface Model (DSM – top-of-canopy). A Canopy

Table 1
LiDAR data collection information for three forests in KwaZulu-Natal, South Africa.

	Date of Acquisition	Scanner	Pulse rate (Hz)	Scan rate (Hz)	Flying height agl (m)	Swath width (m)	Average point density	Ground pixel resolution (cm)	Extent (ha)
Dargle	June 2016	Leica ALS50–2	149 000	54	850	480	10	25	238
Karkloof	17 & 18 June 2018	Leica ALS70	150400	63.3	900	580	12	10	2080
Umgano	14 June 2018	Leica ALS70	150400	63.3	900	580	12	10	157

Height Model (CHM) was then created by subtracting the DEM from the DSM. The DEM and DSM are triangulated models created using linear interpolation of ground and surface returns respectively.

2.4. Mapping aboveground carbon

The circular field plots were mapped on the CHM dataset and mean top of canopy height was extracted for each plot in ArcGIS 10.1. This value was then regressed against field estimated AGC in order to estimate AGC from the LiDAR dataset. Next, a grid of 0.28 ha was used to divide the LiDAR dataset, to match the field data plot size, and mean top of canopy height was then extracted from the CHM for each grid cell. The relationship between the field estimated AGC, and LiDAR mean top of canopy height, further referred to as the local model, was then used to estimate AGC across the entire forest. This was done for each of the three forests, for each allometric equation (Eqs. 1, 2, 3). Data from the three forests was then used to create a single multi-site model to predict the AGC from the LiDAR CHM using a linear mixed effects model (LMM) with forest being included as a random effect. All analyses were run in R vers 4.2.1, the LMM was run using the 'lmer' function from the 'lme4' package (Bates et al., 2015; R Core Team, 2018). A LMM was used to test for differences between the different allometric equations with forest, model (local/multi-site) and source (field/LiDAR) included as random effects. Relationships were significant (Table 2); however, these results are not ecologically meaningful as the large sample sizes from the LiDAR data result in significant values (Kitchin, 2014) even though the standard deviations overlap, therefore differences were assessed qualitatively.

Aboveground carbon values for each forest were also compared to two globally derived aboveground biomass (AGB) products to assess the suitability of such products for mapping carbon in these Afrotemperate forests. The National Centre for Earth Observation (NCEO) Africa Aboveground Woody Biomass (AGB) product for the year 2017 (Rodriguez-Veiga and Balzter, 2021) has a 100 m spatial resolution, and was developed using a combination of satellite data including NASA's Global Ecosystem Dynamics Investigation (GEDI – spaceborne LiDAR), JAXA's L-band SAR ALOS-2 PALSAR-2 mosaics (RADAR) and Landsat Percent Tree Cover (PTC) (Optical remote sensing; (Hansen et al., 2013)). The JPL 2020 Global Biomass Product has a 100 m spatial resolution was derived from a combination of Landsat 8 composite images, JAXA's L-band SAR ALOS-2 PALSAR-2 mosaics, and SRTM DEM data. The model was created using training data from ICESAT-1 (spaceborne LiDAR), airborne LiDAR and field inventory data (https://ceos.org/gst/jpl-biomass.html). Data were extracted for each of the three forests to measure the mean and standard deviation in values for each forest. Biomass was converted to carbon using the same conversion factor of 0.47 (Martin and Thomas, 2011).

3. Results

The relationship between diameter and height is the weakest in the Dargle forest (R^2 =0.33), with dbh ranging from 7 to 126 cm and tree height peaking at 26 m (Fig. 2a). Dargle shows the highest standard error in diameter values (0.75), compared to Karkloof (0.24) and Umgano (0.66). The majority of trees in Karkloof had a dbh < 60 cm, with very few trees > 80 cm (dbh range 3.5 – 103 cm), and no trees > 25 m in height. Trees in Umgano were the largest and tallest compared to other sites, with dbh up to 159 cm, and trees up to 35 m tall. This old growth site shows the best D:H relationship with 86.3% of the variation explained.

Although Dargle has the weakest D:H relationship, the site displays the strongest relationship between field measured AGC and LiDAR estimated mean canopy height (R^2 >0.72 for each type of allometry used) and the lowest RMSE (RMSE < 12 MgC.ha^{-1}) (Table 2). Karkloof has the weakest relationship (R^2 = 0.16–0.26; Table 2) and although the RMSE is comparable to Umgano (44–58 MgC.ha^{-1} in Karkloof, and 38–48 MgC.ha^{-1} in Umgano; Table 2), it is relatively higher (43–65% in Karkloof versus 18–33% in Umgano; Table 2). The multi-site model produces a stronger or similar fit to Karkloof and Umgano if using the marginal pseudo R^2 which includes only the fixed effects, and shows a stronger fit than all other models when the random effect of forest is taken into account with the condition pseudo R^2 (Table 2). The relative

Table 2
Model estimates, R^2, and RMSE for the local models created to estimate aboveground carbon (AGC) from mean canopy height (MCH) measured from LiDAR images over three Afrotemperate forests in KwaZulu-Natal, South Africa using the equation AGC = b_1(MCH) + c. Aboveground carbon was calculated using three different allometric equations (Chave et al., 2014; Coomes et al., 2002; Mensah et al., 2016). Marginal (R^2m) and conditional (R^2c) pseudoR^2 are reported for the multi-site models as they were run using linear mixed effects models.

		Allometry	b_1	c	R^2		RMSE (MgC.ha^{-1})	RMSE (%)
Local	**Dargle**	**Coomes**	0.0503	1.1905	0.7184		11.02	9.72
		Mensah	0.0569	1.1214	0.7451		9.80	7.80
		Chave	0.0571	1.1745	0.7305		10.46	7.27
	Karkloof	**Coomes**	0.0214	1.7343	0.1557		57.56	64.48
		Mensah	0.0279	1.6893	0.2417		46.57	50.00
		Chave	0.0291	1.7232	0.2564		44.85	43.40
	Umgano	**Coomes**	0.0386	1.5251	0.567		47.82	32.65
		Mensah	0.0454	1.4927	0.6104		39.18	22.18
		Chave	0.0482	1.5077	0.6169		38.01	18.61
Multi-site					**R^2m**	**R^2c**		
		Coomes	0.0342	1.5566	0.5610	0.7595	38.40	33.75
		Mensah	0.0414	1.5003	0.5951	0.8151	30.30	23.64
		Chave	0.0329	1.6728	0.6063	0.8173	29.57	20.25

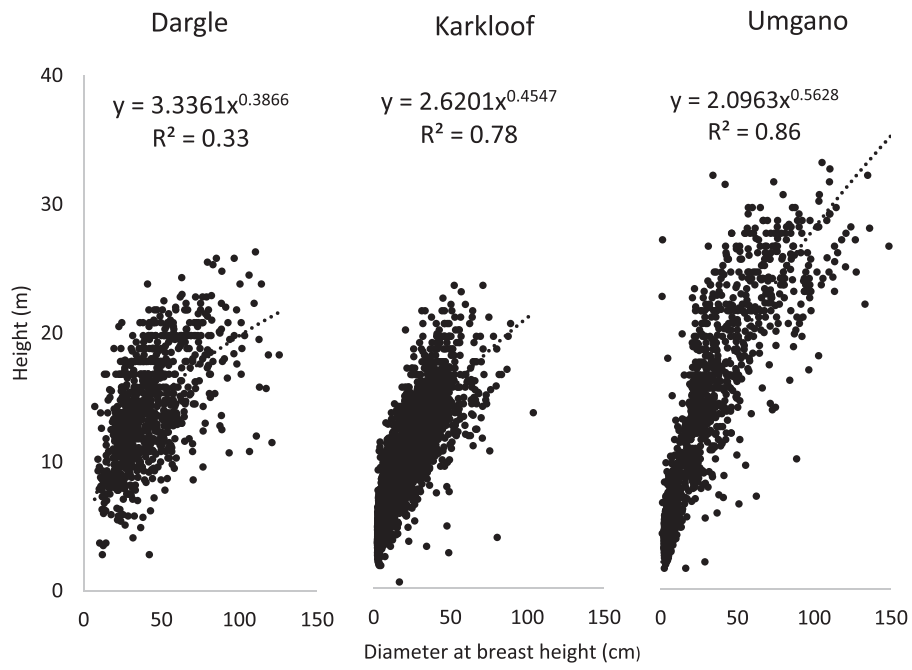

Fig. 2. Diameter height relationships for trees in a. Dargle (n = 902), b. Karkloof (3737) and c. Umgano (n = 1727) forests, KwaZulu-Natal, South Africa.

RMSE for each allometric is also lower for the multi-site model compared to the local model for Karkloof, and similar to the RMSE percentage for Umgano (Table 2).

LiDAR estimated AGC for the entire forest patch, for each forest, resulted in lower overall AGC estimates than those applied to field data (Fig. 3). Regardless of allometry, Karkloof forest consistently has the lowest AGC (82 – 103 MgC.ha^{-1}; Fig. 3, Fig. 4). The majority of the forest is below 100 MgC.ha^{-1}, with the few high AGC pixels resulting from exotic pines (pers. obs.; Fig. 4d). Karkloof is the largest forest mapped in this study, and has the greatest variation in vegetation structure across its extent (Fig. 4c.). Umgano has the highest measures of AGC when calculated using local models (146 – 204 MgC.ha^{-1}; Fig. 3), but estimates are more similar to the AGC stored in Dargle forest when using the multi-site model (Fig. 3). When observing the AGC estimates spatially as calculated using the Mensah et al. (2016) allometry from local models, it becomes even more apparent that the AGC in Karkloof is lower than the other two forests, and this is consistent across the entire forest patch (Fig. 4d) with 93.52% of grid cells in Karkloof containing less than 100 MgC.ha^{-1} (Fig. 5). Dargle and Umgano show a greater number of pixels with high AGC with almost 50% of Umgano, and 12%

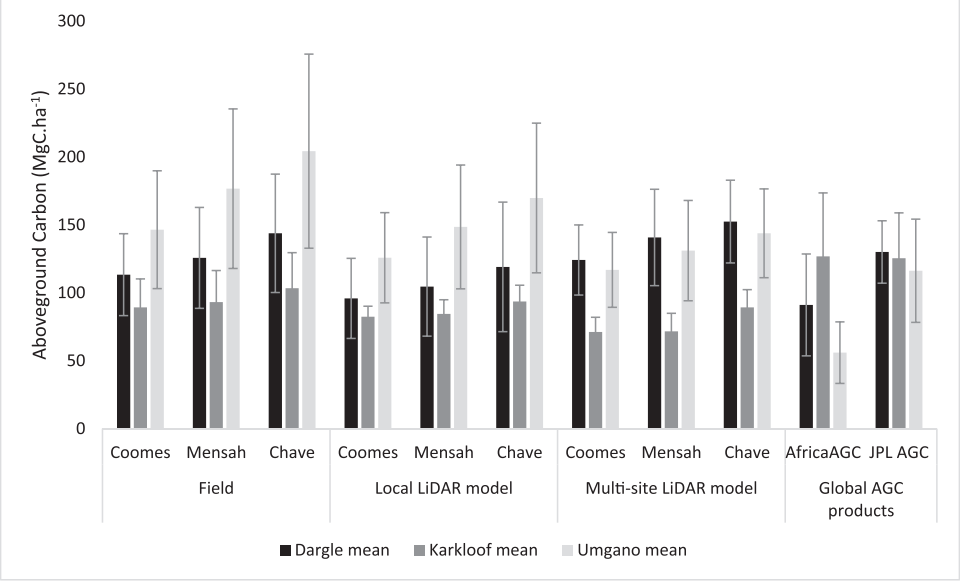

Fig. 3. Mean aboveground carbon (AGC) for three forests in KwaZulu-Natal, South Africa calculated using three different allometric equations (Chave et al., 2014; Coomes et al., 2002; Mensah et al., 2016) as calculated from field plot data (Dargle n = 14, Karkloof n = 16, Umgano n = 13) and estimated from LiDAR data (Dargle n = 665, Karkloof n = 5892, Umgano n = 404) using a local and multi-site model. Mean AGC was also calculated from two global biomass products, the NCEO Africa Aboveground Woody Biomass Product (AfricaAGC) and the JPL 2020 Global Biomass Product (JPL AGC). Error bars denote standard deviation.

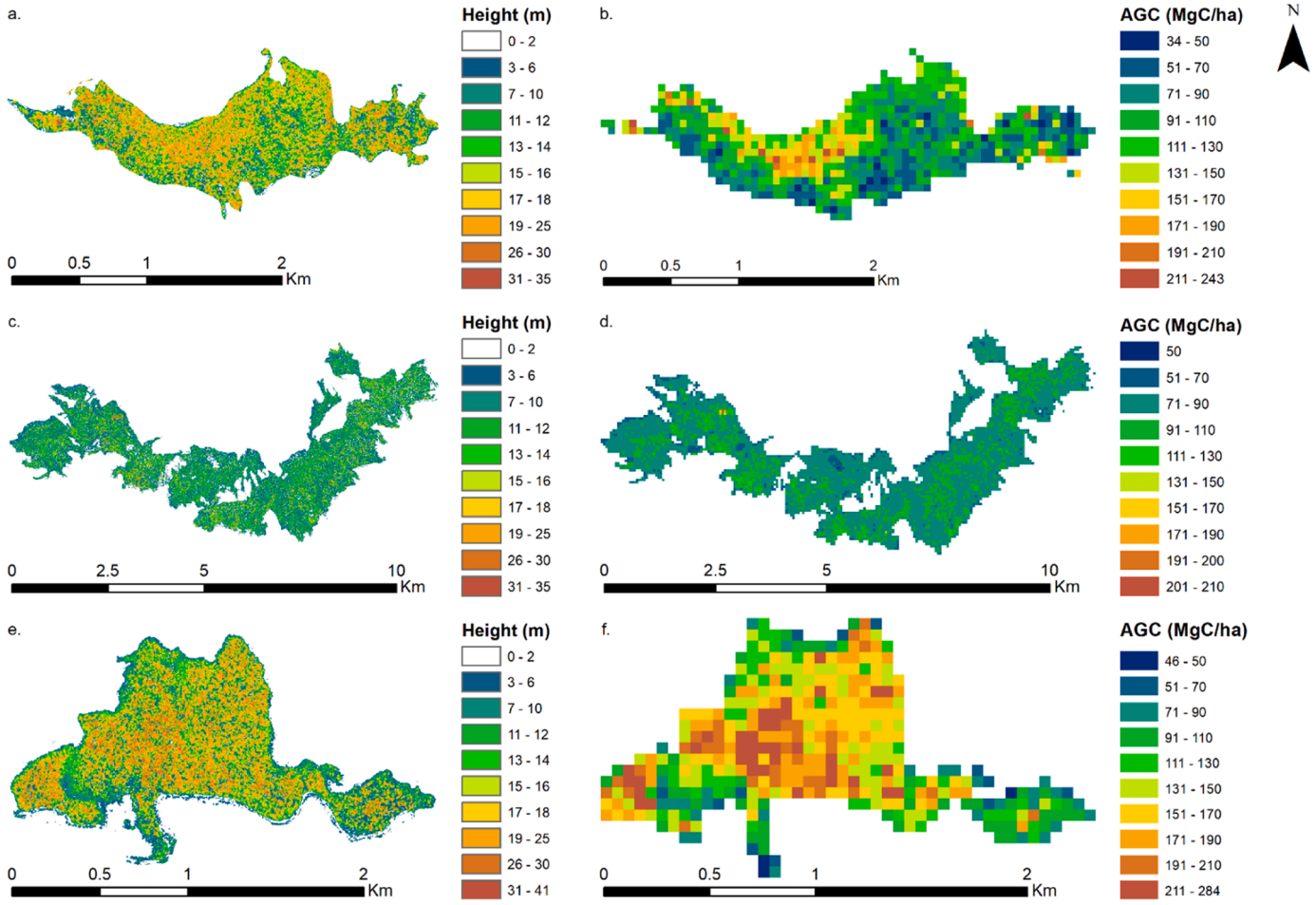

Fig. 4. Maps of mean canopy height (m) and aboveground carbon (AGC; Mg C ha^{-1}) distribution for Dargle forest (a, b), Karkloof forest (c, d) and Umgano forest (e, f) in KwaZulu-Natal, South Africa. Canopy height maps are at a 1 m resolution, and AGC maps are at a 0.28 ha resolution.

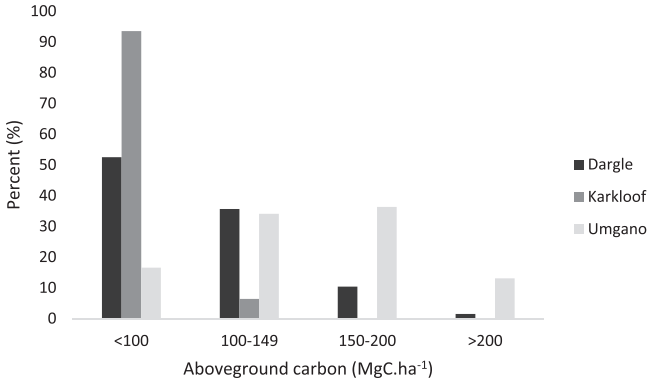

Fig. 5. Percent contribution of 0.28 ha grid cells to four aboveground carbon categories in three forests in KwaZulu-Natal, South Africa.

of Dargle forest containing more than 150 MgC.ha^{-1} (Fig. 4d, f; Fig. 5). In Dargle forest the areas with higher AGC are towards the northern section of the forest which occurs on the steepest slopes, and in Umgano the higher AGC areas are concentrated in the centre of the forest with lower AGC around the edges, particularly in the eastern section of the forest (Fig. 4b,f).

When using the multi-site model, AGC estimates for Karkloof remained similar to those obtained using a local model; however, Dargle was estimated to have more AGC than Umgano for each of the three allometries (Fig. 3). Across forest sites, the lowest AGC was consistently calculated using the Coomes et al. (2002) allometry, and the highest using Chave et al. (2014) (Fig. 3). Both global biomass products overestimate the amount of AGC in Karkloof forest (Fig. 3). The estimates given by the JPL product is more similar to the multi-site LiDAR models for Dargle and Umgano forest, while the NCEO Africa AGC product underestimates the carbon in both of those forests (Fig. 4).

4. Discussion

The accuracy of mapping aboveground carbon in Afrotemperate forests using a multi-site LiDAR model is approximately 24% (30 MgC. ha^{-1}; Table 2), falling within the range reported in other studies (Coops et al., 2021). Local LiDAR models exhibit greater variability in RMSE values with Dargle and Umgano having lower RMSEs than the standard deviation in AGC values, while Karkloof has the opposite result, indicating a higher margin of error in AGC predictions for Karkloof. The high spatial variability of topography and vegetation within Karkloof, the largest forest included in the study, leads to low R^2 and relatively high RMSEs. In addition, the site has high intra-forest variability of tree structure and composition (pers. obs.), indicating different trajectories of regrowth post-logging. While the multi-site LiDAR model is more appropriate for mapping carbon across a large extent of Afrotemperate forests, the high structural variability across forest patches should be considered when interpreting the results. The LiDAR estimated AGC from the multi-site model remains comparable to the local model only for Karkloof forest. For Dargle and Umgano, the AGC is overestimated and underestimated respectively, indicating that variation in AGC per forest patch is lost when using large extent AGB maps. This issue is often

observed in other studies covering large extents (Araza et al., 2022; Réjou-Méchain et al., 2019).

Karkloof had the lowest AGC, followed by Dargle and Umgano. Although logging in both Karkloof and Dargle forests is estimated to have ended around the 1890 s, Dargle exhibits higher AGC (Figs. 3, 4). The higher carbon in Dargle is not uniformly distributed throughout the forest, with taller trees, and thus higher AGC, in the north-west of the forest. The lower AGC towards the edges of the forest could be a result of the forest expanding over time due to fire suppression as the southern border of the forest is surrounded by commercial timber plantations where fires are excluded. Alternatively, the edges could be showing signs of degradation, but would need to be investigated using historical imagery to confirm this (Lawes and Eeley, 2000). Given the location of the timber plantations, and the forest being protected through a local conservancy, fire suppression and forest expansion is a more likely scenario (Adie et al., 2017; Geldenhuys, 1994). Karkloof forest has a uniform distribution of low AGC and shows levels of carbon more similar to a degraded forest (Adie et al., 2013). Umgano contained the highest amount of AGC, as expected from an old-growth forest dominated by long-lived podocarps (Adie et al., 2013), although the carbon estimated in this study is lower than the previous measurement by Adie et al. (2013) of 252.7 (193.4–339.6) MgC.ha^{-1}. The differences in AGC values are attributed to a variety of factors including the allometric used, the size and number of field plots, and the relationship between field measured AGC and LiDAR estimated AGC.

Adie et al. (2013) used the Coomes et al. (2002) allometric, which results in the lowest AGC in this study (Table 2), to compare the AGC of five Afrotemperate forest patches in KwaZulu-Natal, South Africa. Adie et al. (2013) chose the Coomes et al. (2002) allometric because of the structural similarities between the Afrotemperate forests studied and the forest in New Zealand where the equation was developed (Beets, 1980). However, the allometric equations used in studies of AGB in African montane forests vary. Chave et al. (2005) developed their AGB allometric by compiling biomass data from 2410 trees across 27 tropical sites in the Americas, Asia, and Oceania, while Chave et al. (2014) updated this work and applied stricter requirements for data to be included. They refined the original dataset used by Chave et al. (2005) and included data from Latin America, the Afro-tropical realm including Madagascar, and Southeast Asia and Australia resulting in 4004 trees. Studies conducted prior to 2014 tend to use Chave et al. (2005), while those conducted after the paper by Chave et al. (2014) was published use the updated allometric equation (Cuni-Sanchez et al., 2021; Imani et al., 2017; Moore et al., 2018; Nyirambangutse et al., 2017). While the updated equation accounts for more variety, Chave et al. (2014) shows that if the variation in diameter-height relationships are accounted for, the pantropical AGB allometries are robust across all sites, including those allometries developed by Chave et al. (2005) and Feldpausch et al. (2012). Although pantropical allometric equations are suitable for multiple locations, studies suggest locally-derived allometric equations should be used where available. Mensah et al. (Mensah et al., 2016) created a biomass allometric for the northern Mistbelt forests in Limpopo province, South Africa. Despite various shortcomings of the Mensah et al. (2016) equation, which include the small sample size (59 trees), the non-destructive method (which was necessary as the forests were conserved), and the limited number of species (four) included, the equation was developed using robust methods and produces realistic results (Mensah et al., 2017, 2016) because of the inclusion of dbh, height and species-specific wood density. In this study, the results produced using different allometric equations (Fig. 3) are not ecologically different from one another, and perform within an expected range of uncertainty in carbon estimates. I recommend using the Mensah et al. (2016) allometric for calculating AGC in South African Afrotemperate forests as the values are intermediate to the ones resulting from the Coomes et al. (2002) and Chave et al. (2014) equations, and the equation was developed in a South African system.

The patterns in AGC for each of the three forests using the local models are consistent regardless of the allometric used (Fig. 3); however, the LiDAR estimated AGC is lower than the field estimated AGC (Fig. 3). This is because of the different sample sizes, where field measured AGC was sampled in 13 – 16 plots within the forests covering 3.7 – 4.5 ha in total per forest, sampling from the interior of forests, and the LiDAR estimated AGC is for the entire forest patch (157 ha in Umgano to >2000 ha in Karkloof (Table 1)). Therefore, the LiDAR estimated AGC captures all the variation in AGC including the edge areas which typically have lower AGC (Fig. 4). Similarly, when using a globally or regionally derived AGB/AGC product such as the NCEO Africa Aboveground Woody Biomass product (Rodriguez-Veiga and Balzter, 2021), AGC values are grossly under-estimated for Umgano forest, and over-estimated for Karkloof (Fig. 3). Likewise, the AGC estimated using the JPL product overestimates carbon in Karkloof but estimates for Dargle and Umgano are more similar to those estimated using the multi-site LiDAR model (Fig. 3). The question that remains though, is what level of accuracy is necessary for measuring these carbon values for reporting on sustainability?

Ultimately there is no answer to this question, rather, when reporting carbon values, it is essential to be transparent about the methods used to derive the values, results should be comparable over time, and error estimates should be included (Araza et al., 2022; IPCC, 2006; Pulles, 2017; UNFCCC Secretariat, n.d.). Design-based sampling error and the parameters used in allometric equations are the greatest sources of error in AGC values (Araza et al., 2022; McGlynn et al., 2022). Remote sensing of forest biomass can reduce the sample-based error by providing biomass/carbon estimates over greater extents (Herold et al., 2019; McGlynn et al., 2022). But what about Afrotemperate forests? The majority of the Afrotemperate forests in South Africa are secondary forests (such as Dargle and Karkloof) but over 70% of them are not protected and are likely to be degraded due to the high density of surrounding human settlements who rely on NTFPs (Non-Timber Forest Products) and harvest from these forest patches. Therefore currently, global biomass products such as NCEO Africa AGB and the JPL AGC will overestimate their AGC contributions, as is the case with Karkloof forest (Fig. 3). The same is likely to be true for Afromontane and Afrotemperate forests in the rest of the continent as they too are surrounded by rural settlements who rely on NTFPs. The NCEO Africa AGB product estimate of 126 MgC.ha^{-1} is 36% greater than the conservative estimate of 81 MgC.ha^{-1} as calculated using the multi-site LiDAR model for Karkloof (Table 2) which is greater than the current RMSE on the multi-site LiDAR model estimate. However, considering the contribution of Afrotemperate forest carbon across South Africa (~270 000 ha) to the global carbon commitments of South Africa in the NDC is only around 1% (21.9 MgC.ha^{-1} (LiDAR model) - 34.01 MgC.ha^{-1} (NCEO model)), when it comes to reporting, this carbon is unlikely to make much of a difference. If we extrapolate these carbon values across all Afromontane forests on the content which span an estimated 71 500 000 ha (White, 1983), the carbon sink would be 5791–9009 MgC.ha^{-1}. While these carbon sinks are unlikely to tip the scale, they are threatened by subsistence use and deforestation, and as such should be prioritized for monitoring.

As more independent datasets consisting of field and LiDAR data are shared for calibration and validation of global biomass products, these products applicability to novel ecosystems will improve over time. Studies such as Chave et al. (2019), McRoberts et al. (2019), and Réjou-Méchain et al. (2019) have demonstrated the importance of these datasets. However, until more such data becomes available, it is advisable to use locally derived remote sensing estimates of aboveground carbon. For Afrotemperate forests in South Africa, Mensah et al.'s (2016) allometry should be applied, while for other afromontane and Afrotemperate forests where a local allometry does not exist, I would advocate for the use of Mensah et al.'s (2016) or Chave 's et al. (2014) allometrics, the latter because it is so widely used and thus values can be compared globally. The multi-site LiDAR model, which has lower error estimates than the Karkloof and Umgano local models, could be used for

forests where LiDAR data is available without concurrent field data, including indigenous forest patches adjoining plantations that are regularly surveyed. Nevertheless, the multi-site LiDAR model should be updated as more field data becomes available and should cover a wider range of conditions and AGC values, including degraded forest patches.

5. Conclusion

The best practice for measuring AGC of Afrotemperate forests is to use the locally derived allometric presented by Mensah et al. (2016). The other allometrics reviewed in this study can still be calculated as all three require dbh, height and species-specific wood density as inputs. Therefore, when conducting field work such as forest inventory or ground validation for remote sensing, it is imperative to collect these measurements and information (species). Mapping of these forests is still difficult as indicated by the low R^2 for Karkloof and Umgano forests because of the structural heterogeneity in vegetation and the steep terrain. Even so, predictions can be improved by pooling datasets (multi-site model) and these predictions will only get better with the addition of more field validation sites, and greater LiDAR coverage. Estimates of mean canopy height from LiDAR data do present limitations in that the values do not account for the variability in the canopy. This variability can be accounted for by using smaller grid cells for calculations; however, this will significantly increase the processing power needed. For the 2023 'Global Stocktake' of AGC, I recommend using values from the JPL AGC product for Afromontane and Afrotemperate forests. For subsequent carbon reports, research and conservation groups should collaborate and contribute towards a national database for forest inventory. These data should then be shared with agencies creating global biomass/carbon products to improve calibration and validation of these forest systems. The cost of LiDAR data does make it prohibitive for operational use, but it should be used for calibration and validation of free remote sensing products such as Sentinel 1 and 2 imagery which can then be used to map AGC in Afromontane and Afrotemperate forests across their entire extent.

Funding

This work was supported by the National Research Foundation, South Africa [grant number: 117983] and the Botanical Trust, South Africa.

Declaration of Competing Interest

The authors declare that they have no known competing financial interests or personal relationships that could have appeared to influence the work reported in this paper.

Data availability

Data will be made available on request.

Acknowledgements

Thank you to CAD mapping who provided LiDAR data for Dargle forest at no charge, and Land Resources International (LRI) for significantly reducing the cost of LiDAR data collection and processing for Karkloof and Umgano forests. Field data were collected with the assistance of Buster Mogonong, Sibongile Zwane, and Caroline Howes. I am grateful to Hylton Adie for the many hours spent in the field collecting data, helping with my tree identification and teaching me about these wonderful forests. Thank you to various landowners who granted me access to their properties to collect these data; and thank you to the anonymous reviewer for your helpful suggestions.

Author contributions

I, Jolene Fisher, am the sole author on the paper. I secured funding for the research, formulated all research questions, analysed all the data and wrote the entire manuscript.

References

A.E. Zanne G. Lopez-Gonzalez D.A. Coomes J. Ilic S. Jansen S.L. Lewis R.B. Miller N.G. Swenson M.C. Wiemann J. Chave Towards a Worldw. wood Econ. Spectr. 2009 doi: 10.5061/dryad.234.

Adie, H., Rushworth, I., Lawes, M.J., 2013. Pervasive, long-lasting impact of historical logging on composition, diversity and above ground carbon stocks in Afrotemperate forest. For. Ecol. Manag. 310, 887–895. https://doi.org/10.1016/j.foreco.2013.09.037.

Adie, H., Kotze, D.J., Lawes, M.J., 2017. Small fire refugia in the grassy matrix and the persistence of Afrotemperate forest in the Drakensberg mountains. Sci. Rep. 7 (1), 10. https://doi.org/10.1038/s41598-017-06747-2.

Ahmed, R., Siqueira, P., Hensley, S., Bergen, K., 2013. Uncertainty of forest biomass estimates in north temperate forests due to allometry: implications for remote sensing. Remote Sens. 5, 3007–3036. https://doi.org/10.3390/rs5063007.

Araza, A., de Bruin, S., Herold, M., Quegan, S., Labriere, N., Rodriguez-Veiga, P., Avitabile, V., Santoro, M., Mitchard, E.T.A., Ryan, C.M., Phillips, O.L., Willcock, S., Verbeeck, H., Carreiras, J., Hein, L., Schelhaas, M.-J., Pacheco-Pascagaza, A.M., da Conceição Bispo, P., Laurin, G.V., Vieilledent, G., Slik, F., Wijaya, A., Lewis, S.L., Morel, A., Liang, J., Sukhdeo, H., Schepaschenko, D., Cavlovic, J., Gilani, H., Lucas, R., 2022. A comprehensive framework for assessing the accuracy and uncertainty of global above-ground biomass maps. Remote Sens. Environ. 272, 112917 https://doi.org/10.1016/j.rse.2022.112917.

Araza, A., Herold, M., de Bruin, S., Ciais, P., Gibbs, D.A., Harris, N., Santoro, M., Wigneron, J.-P., Yang, H., Málaga, N., Nesha, K., Rodriguez-Veiga, P., Brovkina, O., Brown, H.C.A., Chanev, M., Dimitrov, Z., Filchev, L., Fridman, J., García, M., Gikov, A., Govaere, L., Dimitrov, P., Moradi, F., Muelbert, A.E., Novotný, J., Pugh, T. A.M., Schelhaas, M.-J., Schepaschenko, D., Stereńczak, K., Hein, L., 2023. Past decade above-ground biomass change comparisons from four multi-temporal global maps. Int. J. Appl. Earth Obs. Geoinf. 118, 103274 https://doi.org/10.1016/j.jag.2023.103274.

Asner, G.P., Clark, J.K., Mascaro, J., Galindo García, G.A., Chadwick, K.D., Navarrete Encinales, D.A., Paez-Acosta, G., Cabrera Montenegro, E., Kennedy-Bowdoin, T., Duque, Á., Balaji, A., Von Hildebrand, P., Maatoug, L., Phillips Bernal, J.F., Yepes Quintero, A.P., Knapp, D.E., García Dávila, M.C., Jacobson, J., Ordóñez, M.F., 2012. High-resolution mapping of forest carbon stocks in the Colombian Amazon. Biogeosciences 9, 2683–2696. https://doi.org/10.5194/bg-9-2683-2012.

Banda, S.P., Adams, J.B., Rajkaran, A., Johnson, J.L., Raw, J.L., 2021. Chapter 18 - Blue carbon storage comparing mangroves with saltmarsh and seagrass habitats at a warm temperate continental limit, in: Sidik, F., Friess, D.A. (Eds.), Dynamic Sedimentary Environments of Mangrove Coasts. Elsevier, pp. 447–471. https://doi.org/10.1016/B978–0-12–816437-2.00008–2.

Bates, D., Mächler, M., Bolker, B., Walker, S., 2015. Fitting linear mixed-effects models using lme4. J. Stat. Softw. 67 (1), 48. https://doi.org/10.18637/jss.v067.i01.

Beets, P., 1980. Amount and distribution of dry matter in a mature beech/podocarp community. New Zealand J. For. Sci. 10, 395–418.

Bouvet, A., Mermoz, S., Le Toan, T., Villard, L., Mathieu, R., Naidoo, L., Asner, G.P., 2018. An above-ground biomass map of African savannahs and woodlands at 25 m resolution derived from ALOS PALSAR. Remote Sens. Environ. 206, 156–173. https://doi.org/10.1016/j.rse.2017.12.030.

Chave, J., Andalo, C., Brown, S., Cairns, M.A., Chambers, J.Q., Eamus, D., Fölster, H., Fromard, F., Higuchi, N., Kira, T., Lescure, J.-P., Nelson, B.W., Ogawa, H., Puig, H., Riéra, B., Yamakura, T., 2005. Tree allometry and improved estimation of carbon stocks and balance in tropical forests. Oecologia 145, 87–99. https://doi.org/10.1007/s00442-005-0100-x.

Chave, J., Coomes, D., Jansen, S., Lewis, S.L., Swenson, N.G., Zanne, A.E., 2009. Towards a worldwide wood economics spectrum. Ecol. Lett. 12, 351–366. https://doi.org/10.1111/j.1461-0248.2009.01285.x.

Chave, J., Réjou-Méchain, M., Búrquez, A., Chidumayo, E., Colgan, M.S., Delitti, W.B.C., Duque, A., Eid, T., Fearnside, P.M., Goodman, R.C., Henry, M., Martínez-Yrízar, A., Mugasha, W.A., Muller-Landau, H.C., Mencuccini, M., Nelson, B.W., Ngomanda, A., Nogueira, E.M., Ortiz-Malavassi, E., Pélissier, R., Ploton, P., Ryan, C.M., Saldarriaga, J.G., Vieilledent, G., 2014. Improved allometric models to estimate the aboveground biomass of tropical trees. Glob. Change Biol. 20, 3177–3190. https://doi.org/10.1111/gcb.12629.

Chave, J., Davies, S.J., Phillips, O.L., Lewis, S.L., Sist, P., Schepaschenko, D., Armston, J., Baker, T.R., Coomes, D., Disney, M., Duncanson, L., Hérault, B., Labrière, N., Meyer, V., Réjou-Méchain, M., Scipal, K., Saatchi, S., 2019. Ground data are essential for biomass remote sensing missions. Surv. Geophys 40, 863–880. https://doi.org/10.1007/s10712-019-09528-w.

Colgan, M.S., Asner, G.P., Levick, S.R., Martin, R.E., Chadwick, O.A., 2012. Topo-edaphic controls over woody plant biomass in South African savannas. Biogeosci. Discuss. 9, 957–987. https://doi.org/10.5194/bgd-9-957-2012.

Colgan, M.S., Asner, G.P., Swemmer, T., 2013. Harvesting tree biomass at the stand level to assess the accuracy of field and airborne biomass estimation in savannas. Ecol. Appl. 23, 1170–1184. https://doi.org/10.1890/12-0922.1.

Coomes, D.A., Allen, R.B., Scott, N.A., Goulding, C., Beets, P., 2002. Designing systems to monitor carbon stocks in forests and shrublands. For. Ecol. Manag. 164, 89–108. https://doi.org/10.1016/S0378-1127(01)00592-8.

Coomes, D.A., Dalponte, M., Jucker, T., Asner, G.P., Banin, L.F., Burslem, D.F.R.P., Lewis, S.L., Nilus, R., Phillips, O.L., Phua, M.-H., Qie, L., 2017. Area-based vs tree-centric approaches to mapping forest carbon in Southeast Asian forests from airborne laser scanning data. Remote Sens. Environ. 194, 77–88. https://doi.org/10.1016/j.rse.2017.03.017.

Coops, N.C., Tompalski, P., Goodbody, T.R.H., Queinnec, M., Luther, J.E., Bolton, D.K., White, J.C., Wulder, M.A., van Lier, O.R., Hermosilla, T., 2021. Modelling lidar-derived estimates of forest attributes over space and time: a review of approaches and future trends. Remote Sens. Environ. 260, 112477 https://doi.org/10.1016/j.rse.2021.112477.

R. Core Team, 2018. R: A language and environment for statistical computing. R Foundation for Statistical Computing, Vienna, Austria. URL ⟨https://www.R-project.org/⟩.

Corlett, R.T., 1994. What is secondary forest? J. Trop. Ecol. 10, 445–447.

Cuni-Sanchez, A., Sullivan, M.J.P., Platts, P.J., Lewis, S.L., Marchant, R., Imani, G., Hubau, W., Abiem, I., Adhikari, H., Albrecht, T., Altman, J., Amani, C., Aneseyee, A. B., Avitabile, V., Banin, L., Batumike, R., Bauters, M., Beeckman, H., Begne, S.K., Bennett, A.C., Bitariho, R., Boeckx, P., Bogaert, J., Bräuning, A., Bulonvu, F., Burgess, N.D., Calders, K., Chapman, C., Chapman, H., Comiskey, J., de Haulleville, T., Decuyper, M., DeVries, B., Dolezal, J., Droissart, V., Ewango, C., Feyera, S., Gebrekirstos, A., Gereau, R., Gilpin, M., Hakizimana, D., Hall, J., Hamilton, A., Hardy, O., Hart, T., Heiskanen, J., Hemp, A., Herold, M., Hiltner, U., Horak, D., Kamdem, M.-N., Kayijamahe, C., Kenfack, D., Kinyanjui, M.J., Klein, J., Lisingo, J., Lovett, J., Lung, M., Makana, J.-R., Malhi, Y., Marshall, A., Martin, E.H., Mitchard, E.T.A., Morel, A., Mukendi, J.T., Muller, T., Nchu, F., Nyirambangutse, B., Okello, J., Peh, K.S.-H., Pellikka, P., Phillips, O.L., Plumptre, A., Qie, L., Rovero, F., Sainge, M.N., Schmitt, C.B., Sedlacek, O., Ngute, A.S.K., Sheil, D., Sheleme, D., Simegn, T.Y., Simo-Droissart, M., Sonké, B., Soromessa, T., Sunderland, T., Svoboda, M., Taedoumg, H., Taplin, J., Taylor, D., Thomas, S.C., Timberlake, J., Tuagben, D., Umunay, P., Uzabaho, E., Verbeeck, H., Vleminckx, J., Wallin, G., Wheeler, C., Willcock, S., Woods, J.T., Zibera, E., 2021. High aboveground carbon stock of African tropical montane forests. Nature 596, 536–542. https://doi.org/10.1038/s41586-021-03728-4.

DEFF, (Department of Environment, Forestry and Fisheries), 2020a. National Terrestrial Carbon Sinks Assessment 2020: Technical Report. Pretoria, South Africa.

DEFF, 2020b. Addressing specific elements of REDD+ in South Africa: Comprehensive Assessment of the Definition and Scope of implementation of REDD+ in South Africa. Pretoria (Department of Environment). South Africa. Forestry and Fisheries,.

Dimobe, K., Mensah, S., Goetze, D., Ouédraogo, A., Kuyah, S., Porembski, S., Thiombiano, A., 2018. Aboveground biomass partitioning and additive models for Combretum glutinosum and Terminalia laxiflora in West Africa. Biomass. Bioenergy 115, 151–159. https://doi.org/10.1016/j.biombioe.2018.04.022.

Dubayah, R., Armston, J., Healey, S.P., Bruening, J.M., Patterson, P.L., Kellner, J.R., Duncanson, L., Saarela, S., Ståhl, G., Yang, Z., others, 2022. GEDI launches a new era of biomass inference from space. Environ. Res. Lett. 17, 095001.

Duncanson, L., Kellner, J.R., Armston, J., Dubayah, R., Minor, D.M., Hancock, S., Healey, S.P., Patterson, P.L., Saarela, S., Marselis, S., et al., 2022. Aboveground biomass density models for NASA's Global Ecosystem Dynamics Investigation (GEDI) lidar mission. Remote Sens. Environ. 270, 112845.

Feldpausch, T.R., Lloyd, J., Lewis, S.L., Brienen, R.J., Gloor, M., Monteagudo Mendoza, A., Lopez-Gonzalez, G., Banin, L., Abu Salim, K., Affum-Baffoe, K., others, 2012. Tree height integrated into pantropical forest biomass estimates. Biogeosciences 9, 3381–3403.

H.G. FOURCADE, 1889. Fourcade 1889 Report on the Natal Forests.pdf. PIETERMARITZBURG.

Fransen, T., 2021. Making Sense of Countries' Paris Agreement Climate Pledges.

Geldenhuys, C.J., 1994. Bergwind fires and the location pattern of forest patches in the southern cape landscape, South Africa. J. Biogeogr. 21, 49–62. https://doi.org/10.2307/2845603.

Hansen, M.C., Potapov, P.V., Moore, R., Hancher, M., Turubanova, S.A.A., Tyukavina, A., Thau, D., Stehman, S.V., Goetz, S.J., Loveland, T.R., 2013. High-resolution global maps of 21st-century forest cover change. Science 342, 850–853.

Herold, M., Carter, S., Avitabile, V., Espejo, A.B., Jonckheere, I., Lucas, R., McRoberts, R. E., Næsset, E., Nightingale, J., Petersen, R., Reiche, J., Romijn, E., Rosenqvist, A., Rozendaal, D.M.A., Seifert, F.M., Sanz, M.J., De Sy, V., 2019. The role and need for space-based forest biomass-related measurements in environmental management and policy. Surv. Geophys 40, 757–778. https://doi.org/10.1007/s10712-019-09510-6.

Imani, G., Boyemba, F., Lewis, S., Nabahungu, N.L., Calders, K., Zapfack, L., Riera, B., Balegamire, C., Cuni-Sanchez, A., 2017. Height-diameter allometry and above ground biomass in tropical montane forests: insights from the Albertine Rift in Africa. PLOS ONE 12, e0179653. https://doi.org/10.1371/journal.pone.0179653.

IPCC, 2006, 2006. IPCC guidelines for national greenhouse gas inventories. IGESJapan.

Johnson, J.L., Raw, J.L., Adams, J.B., 2020. First report on carbon storage in a warm-temperate mangrove forest in South Africa. Estuar. Coast. Shelf Sci. 235, 106566.

Kim, R., Kim, D., Cho, S., Choi, E., Park, J., Lee, S.K., Son, Y., 2021. Assessment of REDD + MRV capacity in developing countries and implications under the Paris Regime. Land 10, 943. https://doi.org/10.3390/land10090943.

Kitchin, R., 2014. Big Data, new epistemologies and paradigm shifts. Big Data Soc. 1, 2053951714528481 https://doi.org/10.1177/2053951714528481.

Lawes, M.J., Eeley, H.A.C., 2000. Where have all the forests gone? A brief history of forest use in KwaZulu-Natal. African Wildlife 54, 16–19.

Lawes, M.J., Joubert, R., Griffiths, M.E., Boudreau, S., Chapman, C.A., 2007. The effect of the spatial scale of recruitment on tree diversity in Afromontane forest fragments. Biol. Conserv. 139, 447–456. https://doi.org/10.1016/j.biocon.2007.07.016.

Lefsky, M.A., Cohen, W.B., Acker, S.A., Parker, G.G., Spies, T.A., Harding, D., 1999a. Lidar remote sensing of the canopy structure and biophysical properties of Douglas-fir western hemlock forests. Remote Sens. Environ. 70, 339–361.

Lefsky, M.A., Harding, D., Cohen, W.B., Parker, G., Shugart, H.H., 1999b. Surface lidar remote sensing of basal area and biomass in deciduous forests of eastern Maryland, USA. Remote Sens. Environ. 67, 83–98.

Lefsky, M.A., Cohen, W.B., Harding, D.J., Parker, G.G., Acker, S.A., Gower, S.T., 2002a. Lidar remote sensing of above-ground biomass in three biomes. Glob. Ecol. Biogeogr. 11, 393–399.

Lefsky, M.A., Cohen, W.B., Parker, G.G., Harding, D.J., 2002b. Lidar remote sensing for ecosystem studies. BioScience 52, 19–30.

Loubota Panzou, G.J., Fayolle, A., Jucker, T., Phillips, O.L., Bohlman, S., Banin, L.F., Lewis, S.L., Affum-Baffoe, K., Alves, L.F., Antin, C., others, 2021. Pantropical variability in tree crown allometry. Glob. Ecol. Biogeogr. 30, 459–475.

Maltamo, M., Packalén, P., Yu, X., Eerikäinen, K., Hyyppä, J., Pitkänen, J., 2005. Identifying and quantifying structural characteristics of heterogeneous boreal forests using laser scanner data. For. Ecol. Manag. 216, 41–50. https://doi.org/10.1016/j.foreco.2005.05.034.

Mangwale, K., Shackleton, C.M., Sigwela, A., 2017. Changes in forest cover and carbon stocks of the coastal scarp forests of the Wild Coast, South Africa. South. For. 79, 305–315. https://doi.org/10.2989/20702620.2016.1255480.

Marshall, A.R., Willcock, S., Platts, P.J., Lovett, J.C., Balmford, A., Burgess, N.D., Latham, J.E., Munishi, P.K.T., Salter, R., Shirima, D.D., Lewis, S.L., 2012. Measuring and modelling above-ground carbon and tree allometry along a tropical elevation gradient. Biol. Conserv. REDD Conserv. 154, 20–33. https://doi.org/10.1016/j.biocon.2012.03.017.

Martin, A.R., Thomas, S.C., 2011. A reassessment of carbon content in tropical trees. PLoS ONE 6, 23533. https://doi.org/10.1371/journal.pone.0023533.

Mascaro, J., Detto, M., Asner, G.P., Muller-Landau, H.C., 2011. Evaluating uncertainty in mapping forest carbon with airborne LiDAR. Remote Sens. Environ. 115, 3770–3774. https://doi.org/10.1016/j.rse.2011.07.019.

McCracken, D.P., 1986. The indigenous forests of Colonial Natal and Zululand. Natalia 16, 19–38.

McGlynn, E., Li, S., F. Berger, M., Amend, M., L. Harper, K., 2022. Addressing uncertainty and bias in land use, land use change, and forestry greenhouse gas inventories. Clim. Change 170, 5. https://doi.org/10.1007/s10584-021-03254-2.

McRoberts, R.E., Næsset, E., Liknes, G.C., Chen, Q., Walters, B.F., Saatchi, S., Herold, M., 2019. Using a finer resolution biomass map to assess the accuracy of a regional, map-based estimate of forest biomass. Surv. Geophys 40, 1001–1015. https://doi.org/10.1007/s10712-019-09507-1.

Mensah, S., Veldtman, R., Du Toit, B., Glèlè Kakaï, R., Seifert, T., 2016. Aboveground biomass and carbon in a South African mistbelt forest and the relationships with tree species diversity and forest structures. Forests 7, 79.

Mensah, S., Veldtman, R., Seifert, T., 2017. Allometric models for height and aboveground biomass of dominant tree species in South African Mistbelt forests. South. For. 79, 19–30. https://doi.org/10.2989/20702620.2016.1225187.

Mensah, S., du Toit, B., Seifert, T., 2018. Diversity–biomass relationship across forest layers: implications for niche complementarity and selection effects. Oecologia 187, 783–795. https://doi.org/10.1007/s00442-018-4144-0.

Mograbi, P.J., Erasmus, B.F.N., Witkowski, E.T.F., Asner, G.P., Wessels, K.J., Mathieu, R., Knapp, D.E., Martin, R.E., Main, R., 2015. Biomass Increases Go under Cover: woody vegetation dynamics in South African Rangelands. PLOS ONE 10, e0127093. https://doi.org/10.1371/journal.pone.0127093.

Moore, E.K., Iason, G.R., Pemberton, J.M., Bryce, J., Dayton, N., Britton, A.J., Pakeman, R.J., 2018. Habitat impact assessment detects spatially driven patterns of grazing impacts in habitat mosaics but overestimates damage. J. Nat. Conserv. 45, 20–29. https://doi.org/10.1016/j.jnc.2018.07.005.

Morsdorf, F., Meier, E., Kötz, B., Itten, K.I., Dobbertin, M., Allgöwer, B., 2004. LIDAR-based geometric reconstruction of boreal type forest stands at single tree level for forest and wildland fire management. Remote Sens. Environ. 92, 353–362. https://doi.org/10.1016/j.rse.2004.05.013.

Mucina, L., Rutherford, M.C., 2006. The vegetation of South Africa, Lesotho and Swaziland. The vegetation of South Africa, Lesotho and Swaziland.

Naidoo, L., Mathieu, R., Main, R., Kleynhans, W., Wessels, K., Asner, G., Leblon, B., 2015. Savannah woody structure modelling and mapping using multi-frequency (X-, C- and L-band) Synthetic Aperture Radar data. ISPRS J. Photogramm. Remote Sens. 105, 234–250. https://doi.org/10.1016/j.isprsjprs.2015.04.007.

Nickless, A., Scholes, R.J., Archibald, S., 2011. A method for calculating the variance and confidence intervals for tree biomass estimates obtained from allometric equations. South Afr. J. Sci. 107, 1–10.

Nyirambangutse, B., Zibera, E., Uwizeye, F.K., Nsabimana, D., Bizuru, E., Pleijel, H., Uddling, J., Wallin, G., 2017. Carbon stocks and dynamics at different successional stages in an Afromontane tropical forest. Biogeosciences 14, 1285–1303. https://doi.org/10.5194/bg-14-1285-2017.

Odipo, V.O., Nickless, A., Berger, C., Baade, J., Urbazaev, M., Walther, C., Schmullius, C., 2016. Assessment of aboveground woody biomass dynamics using terrestrial laser scanner and L-Band ALOS PALSAR Data in South African Savanna. Forests 7, 294. https://doi.org/10.3390/f7120294.

P. Rodriguez-Veiga H. Balzter Afr. Aboveground Biomass-.-. map 2021 2017 doi: 10.25392/leicester.data.15060270.v1.

Parmesan, C., Morecroft, M., Trisurat, Y., Adrian, R., Anshari, G., Arneth, A., Gao, Q., Gonzalez, P., Harris, R., Price, J., others, 2022. Terrestrial and freshwater ecosystems and their services. in: Climate Change 2022: Impacts, Adaptation, and Vulnerability.

Contribution of Working Group II to the Sixth Assessment Report of the Intergovernmental Panel on Climate Change. Cambridge University Press,, Cambridge, UK and New York, NY, USA, pp. 197–377. https://doi.org/10.1017/9781009325844.004.

Ploton, P., Barbier, N., Takoudjou Momo, S., Réjou-Méchain, M., Boyemba Bosela, F., Chuyong, G., Dauby, G., Droissart, V., Fayolle, A., Goodman, R.C., Henry, M., Kamdem, N.G., Mukirania, J.K., Kenfack, D., Libalah, M., Ngomanda, A., Rossi, V., Sonké, B., Texier, N., Thomas, D., Zebaze, D., Couteron, P., Berger, U., Pélissier, R., 2016. Closing a gap in tropical forest biomass estimation: taking crown mass variation into account in pantropical allometries. Biogeosciences 13, 1571–1585. https://doi.org/10.5194/bg-13-1571-2016.

Pulles, T., 2017. Did the UNFCCC review process improve the national GHG inventory submissions? Carbon Manag. 8, 19–31. https://doi.org/10.1080/17583004.2016.1271256.

Réjou-Méchain, M., Barbier, N., Couteron, P., Ploton, P., Vincent, G., Herold, M., Mermoz, S., Saatchi, S., Chave, J., de Boissieu, F., Féret, J.-B., Takoudjou, S.M., Pélissier, R., 2019. Upscaling forest biomass from field to satellite measurements: sources of errors and ways to reduce them. Surv. Geophys 40, 881–911. https://doi.org/10.1007/s10712-019-09532-0.

Rolo, V., Olivier, P.I., Pfeifer, M., van Aarde, R.J., 2018. Functional diversity mediates contrasting direct and indirect effects of fragmentation on below- and above-ground carbon stocks of coastal dune forests. For. Ecol. Manag. 407, 174–183. https://doi.org/10.1016/j.foreco.2017.10.059.

Roxburgh, S.H., Paul, K.I., Clifford, D., England, J.R., Raison, R.J., 2015. Guidelines for constructing allometric models for the prediction of woody biomass: How many individuals to harvest? art38 Ecosphere 6. https://doi.org/10.1890/ES14-00251.1.

Smithwick, E.A.H., 2019. Carbon stocks and biodiversity of coastal lowland forests in South Africa: implications for aligning sustainable development and carbon mitigation initiatives. Carbon Manag. 10, 349–360. https://doi.org/10.1080/17583004.2019.1620035.

Spracklen, D.V., Righelato, R., 2014. Tropical montane forests are a larger than expected global carbon store. Biogeosciences 11, 2741–2754. https://doi.org/10.5194/bg-11-2741-2014.

Steinke, T., Ward, C., Rajh, A., 1995. Forest structure and biomass of mangroves in the Mgeni estuary, South Africa. Hydrobiologia 295, 159–166.

Vepakomma, U., St-Onge, B., Kneeshaw, D., 2008. Spatially explicit characterization of boreal forest gap dynamics using multi-temporal lidar data. Remote Sens. Environ. 112, 2326–2340. https://doi.org/10.1016/j.rse.2007.10.001.

White, F., 1983. The Vegetation of Africa, a descriptive memoir to accompany the UNESCO/AETFAT/UNSO Vegetation Map of Africa. UNESCO, Paris.

Xu, L., Saatchi, S.S., Shapiro, A., Meyer, V., Ferraz, A., Yang, Y., Bastin, J.-F., Banks, N., Boeckx, P., Verbeeck, H., Lewis, S.L., Muanza, E.T., Bongwele, E., Kayembe, F., Mbenza, D., Kalau, L., Mukendi, F., Ilunga, F., Ebuta, D., 2017. Spatial distribution of carbon stored in forests of the democratic Republic of Congo. Sci. Rep. 7 https://doi.org/10.1038/s41598-017-15050-z.

Zhao, K., Suarez, J.C., Garcia, M., Hu, T., Wang, C., Londo, A., 2018. Utility of multitemporal lidar for forest and carbon monitoring: tree growth, biomass dynamics, and carbon flux. Remote Sens. Environ. 204, 883–897. https://doi.org/10.1016/j.rse.2017.09.007.

Zolkos, S.G., Goetz, S.J., Dubayah, R., 2013. A meta-analysis of terrestrial aboveground biomass estimation using lidar remote sensing. Remote Sens. Environ. 128, 289–298. https://doi.org/10.1016/j.rse.2012.10.017.